



Developmental plasticity and stability in the tracheal networks supplying *Drosophila* flight muscle in response to rearing oxygen level



Jon F. Harrison^{a,*}, James S. Waters^{a,b}, Taylor A. Biddulph^a, Aleksandra Kovacevic^{a,c},
C. Jaco Klok^{a,d}, John J. Socha^e

^a School of Life Sciences, Arizona State University, PO Box 874501, Tempe, AZ 85287-4501, USA

^b Department of Biology, Providence College, Providence, RI 02918, USA

^c School of Biological Sciences, Monash University, Clayton, Victoria 3800, Australia

^d Sable Systems International, 3840 N. Commerce St., North Las Vegas, NV 89032, USA

^e Department of Biomedical Engineering and Mechanics, Virginia Tech, 332 Norris Hall, Blacksburg, VA 24061, USA

ARTICLE INFO

Keywords:

Tracheae
Tracheoles
Oxygen
Developmental plasticity
Gas exchange
Flight muscle

ABSTRACT

While it is clear that the insect tracheal system can respond in a compensatory manner to both hypoxia and hyperoxia, there is substantial variation in how different parts of the system respond. However, the response of tracheal structures, from the tracheoles to the largest tracheal trunks, have not been studied within one species. In this study, we examined the effect of larval/pupal rearing in hypoxia, normoxia, and hyperoxia (10, 21 or 40 kPa oxygen) on body size and the tracheal supply to the flight muscles of *Drosophila melanogaster*, using synchrotron radiation micro-computed tomography (SR- μ CT) to assess flight muscle volumes and the major tracheal trunks, and confocal microscopy to assess the tracheoles. Hypoxic rearing decreased thorax length whereas hyperoxic-rearing decreased flight muscle volumes, suggestive of negative effects of both extremes. Tomography at the broad organismal scale revealed no evidence for enlargement of the major tracheae in response to lower rearing oxygen levels, although tracheal size scaled with muscle volume. However, using confocal imaging, we found a strong inverse relationship between tracheole density within the flight muscles and rearing oxygen level, and shorter tracheolar branch lengths in hypoxic-reared animals. Although prior studies of larger tracheae in other insects indicate that axial diffusing capacity should be constant with sequential generations of branching, this pattern was not found in the fine tracheolar networks, perhaps due to the increasing importance of radial diffusion in this regime. Overall, *D. melanogaster* responded to rearing oxygen level with compensatory morphological changes in the small tracheae and tracheoles, but retained stability in most of the other structural components of the tracheal supply to the flight muscles.

1. Introduction

Many insects experience hypoxia during development due to larval or pupal location underground, or within organic material including other animals (Callier et al., 2015; Hoback and Stanley, 2001; Schmitz and Harrison, 2004). Additionally, as juvenile insects develop, growth of oxygen-requiring tissues may lead to localized regions of hypoxia (Callier and Nijhout, 2014), and in some cases, intense aerobic activity or high-altitude environments may also induce tissue hypoxia (Dillon and Dudley, 2014; Harrison et al., 1991; Marden et al., 2012). An emerging body of research has demonstrated that many aspects of the morphology of the tracheal system change in response to hypoxia or

hyperoxia, producing compensatory changes in gas exchange capacity that help ensure appropriate local levels of oxygen (Centanin et al., 2010; Harrison et al., 2006; Henry and Harrison, 2004; Klok et al., 2016; Loudon, 1989; VandenBrooks et al., 2012). The insect tracheal system consists of multiple components that vary greatly in size, including the large (up to 2 mm) multicellular conducting tracheae and the small tracheoles (as small as 90 nm in diameter) that are formed from elaborately branched portions of single tracheolar cells. The relative importance of morphological changes in these different sub-sections of the tracheal system to compensatory responses to varied oxygen remains unclear. To date, no studies have examined the effect of rearing oxygen level on both large tracheal and fine-scale tracheolar supply to

Abbreviations: SR- μ CT, synchrotron radiation micro-computed tomography; RVLfMT, right ventro-lateral flight muscle trachea; P_{O₂}, partial pressure of oxygen; DLfM, dorsal-longitudinal flight muscles

* Corresponding author.

E-mail address: j.harrison@asu.edu (J.F. Harrison).

<http://dx.doi.org/10.1016/j.jinsphys.2017.09.006>

Received 3 May 2017; Received in revised form 16 August 2017; Accepted 9 September 2017

Available online 18 September 2017

0022-1910/ © 2017 Elsevier Ltd. All rights reserved.

an insect tissue. Here, we use two imaging techniques to study structural characteristics of the tracheal system—synchrotron radiation micro-computed tomography (SR- μ CT) to assess the morphology of tracheal structures larger than ten microns in diameter, and confocal microscopy to assess the smaller tracheolar structures. These tools enabled us to examine the integrated morphological responses of the tracheal supply to the flight muscle of *Drosophila melanogaster* reared in hypoxia (10 kPa-O₂), normoxia (21 kPa-O₂), and hyperoxia (40 kPa-O₂).

Insects transport and exchange respiratory gases using a tracheal system of branching and anastomosing, thin-walled, air-filled epithelial tubes. Oxygen enters via (usually) occludable spiracles, and then travels via a branching network of tracheal trunks to the metabolically active tissues throughout an insect's body. The tracheae vary greatly in size, structure, and organization within an individual, between developmental stages, and across the great diversity of insect taxa (Harrison et al., 2013a). The terminal tracheal cells form cytoplasmic extensions (tracheoles), which are blind-ended, air-filled tubes that are considered to range from 90 nm to 2.0 μ m in diameter, the surface areas of which provide the primary sites for respiratory gas exchange between the environment and active tissues (Hartung et al., 2004; Meyer, 1989; Schmitz and Perry, 1999; Snelling et al., 2011; Wigglesworth, 1983). Transport of gases in the insect respiratory system often occurs by both advection and diffusion, though the relative importance of each process across the various components of tracheal networks remains poorly understood (Harrison et al., 2013b; Huang et al., 2014; Scheid et al., 1981; Socha et al., 2010).

It is now well documented that developmental plasticity of the major conducting tracheae can facilitate physiological compensation for variation in ambient oxygen availability; however, there is substantial variation across species and tracheae within species. In the larvae of the beetle *Tenebrio molitor*, the diameter of several major longitudinal tracheae vary such that diffusive capacities perfectly compensate for changing atmospheric oxygen (10–21 kPa) experienced during ontogeny (Loudon, 1989). Conversely, the spiracular tracheae of larval *T. molitor* (Loudon, 1989), and the transverse tracheae of the adult grasshopper, *Schistocerca americana*, show no changes in morphology when reared at 5–40 kPa O₂ (Harrison et al., 2006). In general, intermediate, partial compensatory changes are the most common response. Compensatory changes (smaller diameters in hyperoxia, larger diameters in hypoxia) occur for leg and abdominal tracheae of adult *D. melanogaster* (Klok et al., 2016), the dorsal-longitudinal tracheae of *D. melanogaster* larvae (Henry and Harrison, 2004), and the sub-cuticular abdominal tracheae of the larval lepidopteran, *Calpododes ethlius* and the larval hemipteran, *Rhodnius prolixus* (Locke, 1958). Although piecemeal, these studies provide some basis to support the hypothesis that distal tracheae, which may be less effectively ventilated (e.g. leg tracheae), exhibit more morphological variation than tracheae located near spiracles that may be more easily ventilated. Diversity in responses across insects and tracheae might occur because some tracheae may have primarily diffusion-based gas exchange and strong compensatory morphological response, whereas others may exhibit stronger ventilatory responses to atmospheric oxygen and thus may not require morphological compensation.

Insect tracheoles can also exhibit compensatory responses to rearing oxygen level. Hypoxia stimulates greater branching and density of tracheoles, whereas hyperoxia reduces tracheolar density (Jarecki et al., 1999; Locke, 1958; Wigglesworth, 1983). Oxygen-mediated developmental responses of tracheae and tracheoles result from hypoxia-inducible factor (HIF)-mediated control of growth factor pathways (Acevedo et al., 2010; Centanin et al., 2010; Jarecki et al., 1999; Lavista-Llanos et al., 2002). While we know that both the tracheae and the number of tracheoles can respond in a compensatory fashion to varied oxygen availability, we currently lack the information necessary to estimate how effective this compensation is, as we lack quantitative information on how hypoxia or hyperoxia affect the diameter, length, and diffusing capacities of the entire tracheal supply to a tissue.

The physiology of flying *D. melanogaster* is particularly well known among insects, facilitating analysis of gas exchange through the flight muscle tracheal system. As for other insects, oxygen consumption rate increases dramatically during flight, mostly due to the activity of the flight muscles, allowing estimation of flight-muscle-specific oxygen consumption rate (Dickinson and Lighton, 1995). *Drosophila melanogaster* is one of the very few insects for which maximal flight oxygen consumption rate has been determined (Lehmann and Dickinson, 1997). The gas transport capacities of the thoracic spiracles, estimated from water vapor flux, maintain low gradients (\sim 1 kPa) for oxygen diffusion across the spiracle; therefore, we know that during flight, P_{O₂} in the major trachea should be about 19.9 kPa (Lehmann, 2001). Despite the small gradient for oxygen across the spiracles, blocking even a single thoracic spiracle significantly reduces flight power, demonstrating that there is little safety margin for oxygen delivery (Heymann and Lehmann, 2006). Given the small oxygen gradient across the spiracles, lower conductance steps must occur elsewhere within the tracheal system. During flight, *D. melanogaster* circulate hemolymph within the body cavity and potentially air within the tracheal system of their thorax using a pumping proboscis (Lehmann and Heymann, 2005; Westneat et al., 2008), so oxygen transport to the flight muscle results from both diffusion and bulk flow of air. In contrast to adults, larval *Drosophila* may experience hypoxia, as the culture medium becomes strongly anoxic during development (Callier et al., 2015). However, as late-instar larvae breathe using abdominal spiracles held near the medium-air interface, they may be substantially protected from this type of hypoxia. Despite research spanning more than a century with *D. melanogaster* used as a model organism in biology, only the major tracheal trunks and air sacs of the tracheal system in the thorax of *D. melanogaster* have been previously described (Whitten, 1957). Here, we investigated how the structure of the tracheal supply of adult *D. melanogaster* to the dorsal-longitudinal flight muscles (DLFM) is affected by the partial pressure of oxygen experienced during development, combining the measurement approaches of SR- μ CT and confocal microscopy, allowing us to examine tracheal structures from the large conducting tracheae to the small tracheoles. A central hypothesis tested, based on the prior comparative studies, was that most morphological compensation will occur in the small, distal tracheae and tracheoles, rather than in the large, likely well-ventilated primary and secondary tracheae.

2. Methods

2.1. Animals and general conditions

Approximately 80 1–3 day old adult *D. melanogaster* (Oregon R strain) taken from lab cultures maintained as previously described (Klok et al., 2009) were placed into 237 ml plastic bottles with 50 ml of yeast media to lay eggs for 24 h. These eggs were then transferred at equal, low densities (50–100 eggs per 237 ml bottle) to chambers that were regulated at 10, 21, or 40 kPa oxygen environments using a controller that monitored and adjusted chamber oxygen level every few minutes (ROXY-8, Sable Systems) to regulate the oxygen partial pressure in each chamber (Klok et al., 2009). The oxygen chambers were kept in a walk-in environmental room maintained at 24.5 °C. Adults were removed daily and transferred to a new vial containing standard media. Males used for confocal microscopy were four days past eclosion.

For SR- μ CT work, adult flies were placed in fresh vials to lay eggs for 2 h and then removed in order to synchronize larval development. Once the larvae reached the second instar, the vials were packed in Teflon bags filled with 10, 21 or 40 kPa oxygen atmospheres. Immediately upon sealing the bags, they were overnight shipped in a thermally insulated box from Arizona State University to Argonne National Laboratory. Upon arrival, the bags were re-perfused with the required oxygen mixtures from premixed compressed cylinders (during

the < 24 h shipping time oxygen levels did not change by more than 2 kPa in any of the test atmospheres). Larval development progressed through three instars to pupation, and adult males were imaged with SR- μ CT 1–4 days after eclosion.

2.2. Synchrotron radiation micro-tomography (SR- μ CT)

The SR- μ CT imaging of *D. melanogaster* was performed at the Advanced Photon Source in Argonne National Laboratory using the 2-BM-B beamline following previously described methods for imaging insect tracheae (Socha and DeCarlo, 2008). The X-ray energy was set to 15 keV with a 100 mm distance between the sample and the cerium-doped LuAG scintillator, and a 10 \times lens. Flies were killed with fumes of ethyl acetate, and then mounted for imaging in a 2 mm diameter polyimide tube (Kapton, Dow). To help reduce tissue movement, samples were stored at 4 °C, and then taken out 30 min prior to imaging to equilibrate to room temperature. Images were recorded with an exposure time of 375 ms using a 2048 \times 2048 pixel cooled CCD sensor (CoolSNAP, Photometrics) as the sample was rotated 180° around the vertical axis, one image every 0.125°, for a total of 1440 projection images recorded per sample. The field of view for each image was approximately 1.5 \times 1.5 mm with a pixel size of 0.74 μ m, calibrated with a 400 lines per inch gold mesh grid.

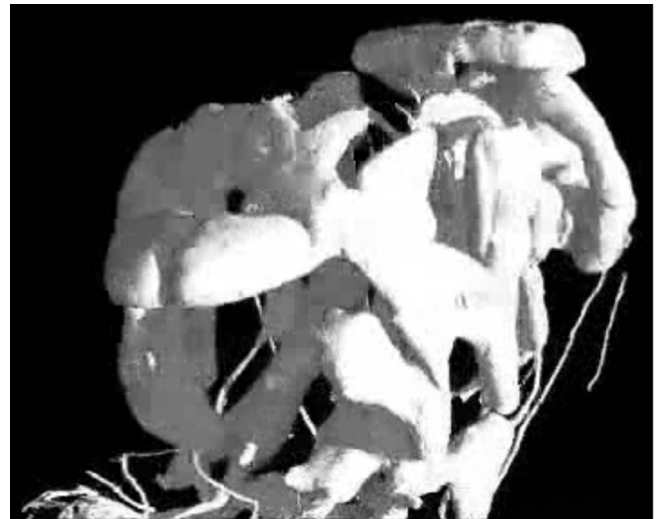
2.3. SR- μ CT image analysis

Image reconstructions were computed using the Gridrec routine (Dowd et al., 1999) at the Advanced Photon Source and the slices saved as HDF files. These images were converted to TIFF format and imported into Avizo Fire 7.0 for analysis. The three-dimensional volumetric data were visualized (Fig. 1A and B) using an isosurface rendering tool at a threshold value of 128 (on a scale of 0–255). We analyzed data for a total of 29 flies (9 reared in 10 kPa, 11 in 21 kPa, and 9 in 40 kPa oxygen).

We focused our quantitative analysis on the branches of the primary tracheal trunk that we designate as the right ventro-lateral flight muscle trachea (RVLfMT), based on its location and tissues serviced (Fig. 1C–E). The RVLfMT was easily identifiable across individuals. The RVLfMT extends from the second spiracle on the right side of the thorax to the four ventral-most DLFM; it appears to serve approximately half of the volume of these cells, with the remaining tracheal supply coming from the parenteric air sacs and interior central tracheae (Fig. 1, Supplemental Movies 1 and 2). The volume of tissue surrounding the RVLfMT tracheal branch was virtually partitioned from the remainder of the thorax (Fig. 1C–F).



Supplemental movie 1. Movie of a rotating *Drosophila melanogaster*, showing the air sacs, reconstructed from SR- μ CT, from all angles.



Supplemental movie 2. Movie of a rotating *Drosophila melanogaster*, showing the tracheal system of the thorax, reconstructed from SR- μ CT. The RVLfMT ascends from the spiracle along the side of the longitudinal muscle; the main trunk is not strictly cylindrical, and the variation in its shape and state of deformation among individuals suggests that it may be compressible (Fig. 1D and E). As the primary trunk varied greatly in size and shape among individuals, we did not quantitatively analyze its morphology. We defined as secondary inter-fiber branches of the RVLfMT the three groupings of tracheae that branched perpendicularly from the main trunk, penetrating between the muscle fibers designated as 1, 2, 3 and 4 in Fig. 1C. We defined as secondary side branches of the RVLfMT any branches from the primary trunk that were not grouped spatially with the inter-fiber branches; most of these directly penetrated muscle fibers from the primary branch. Tertiary branches were defined as tracheal branches that branched approximately perpendicularly from the secondary branches and penetrated the muscle fibers. While the secondary and tertiary tracheae could be compressible, they appeared similar in shape across individuals and these were likely not collapsed. Average diameter of the tertiary tracheae was about 10 μ m, and voxel size was 0.7 μ m. We counted the number of branches manually (1070 branches total), rotating the volumetric data to observe all of the tracheae. We calculated the total length, number of segments, and average length of all tracheae using the autoskeleton function in Avizo. After digitally removing the primary trunk (Fig. 1D), we measured the volume of the secondary and tertiary branches of the RVLfMT using the material statistics module to test for changes in the dimensions of the summed network of branching tracheae.

To assess possible effects of the oxygen-rearing environment on the flight muscles, we measured volumes of the four dorso-longitudinal muscles on the right side of the body served by the RVLfMT (numbers 1–4 in Fig. 1C). These muscles were identified using the orthoslice module, which provided a two-dimensional grayscale cross-sectional view of the specimens, and were traced using the Segmentation Editor. The outline of each individual fiber was traced every 100 image slices (each data stack composed of 2048 \times 2048 \times 2048 voxels) for the entire length of the fiber, and the Interpolation tool was used to label the muscle tissue between these slices. Once the entire outline of the muscle cell was identified, the material statistics module was used to calculate the volumes of the flight muscle fibers. For one fly reared at 21 kPa oxygen, we highlighted air sacs by manual segmentation to illustrate this system (Fig. 2).

2.4. Confocal microscopy

Flies were cold anesthetized and dissected in preparation for imaging. The head and abdomen were discarded and the thorax bisected

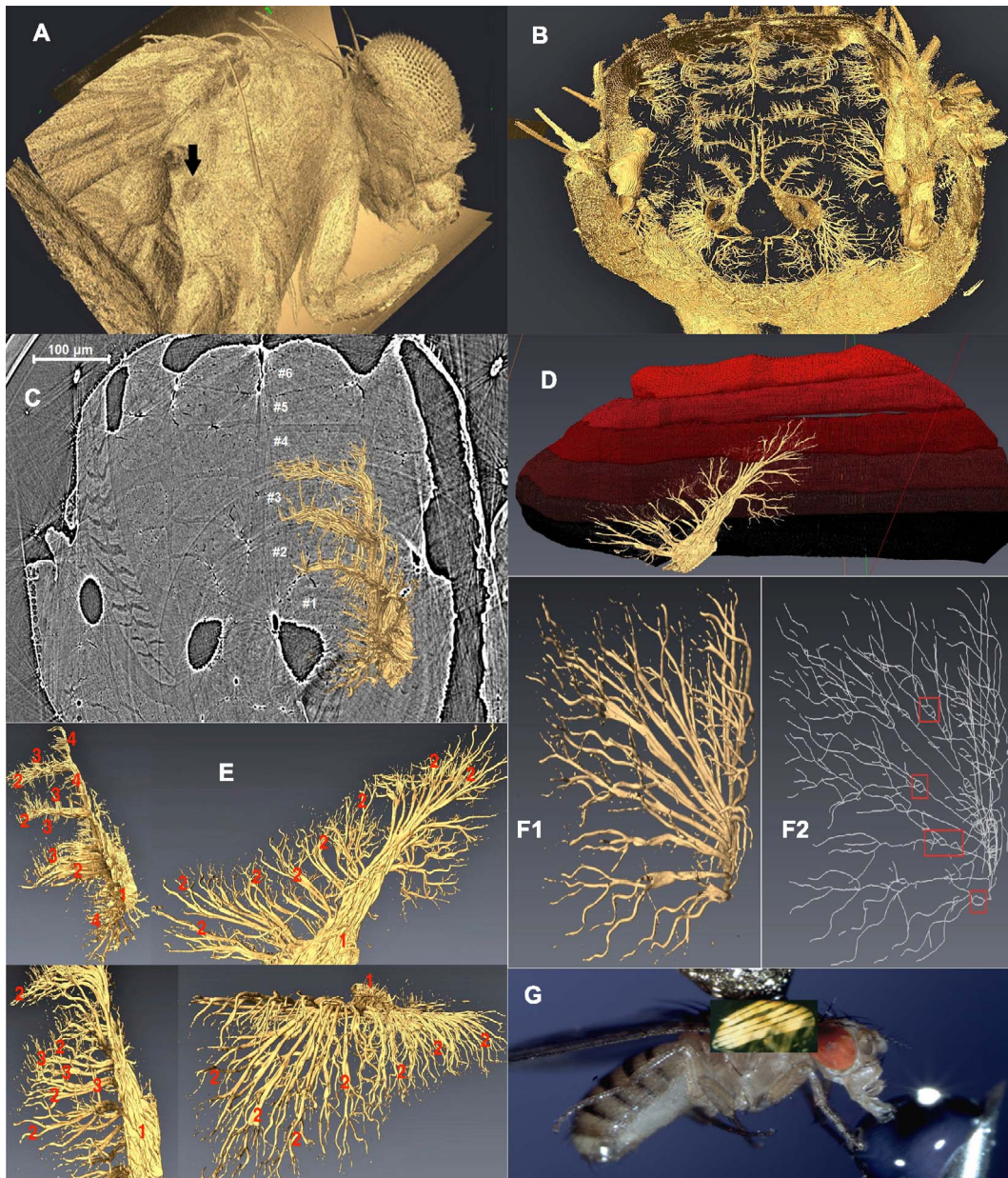


Fig. 1. SR- μ CT images of *Drosophila melanogaster*. A. 3D isosurface rendering of the head and thorax, showing the location of the 2nd spiracle. B. Cross-section of the thorax, using an isosurface rendering to show the tracheal system. Most of the dorsal central region is space occupied by the dorsal-longitudinal flight muscle (DLFM). While the muscle cannot be viewed in this image, the roughly rectangular shapes outlined by the tracheae in this region are spaces occupied by cells of the DLFM. C. Orthoslice coronal plane of the thorax combined with a 3D volume rendering of the right ventro-lateral flight muscle tracheae (RVLFTM), showing the numbering of the DLFM. D. Lateral view the volume rendered DLFM and the RVLFTM. E. Four different views of the RVLFTM, with the primary, secondary and tertiary branches labeled. F1. A component of the RVLFTM and F2, the same trachea as rendered by the autoskeleton function. Red squares indicate examples of false loops created by the autoskeleton function, which were generally small, and so we believe these did not cause a major error. G. Image of live fly combined with a superimposed isosurface-rendered image of the DLFM.

along the antero-posterior axis from the notum to the sternum with fine scissors and a scalpel. The digestive tract was removed and the remaining muscle tissue of the thorax was fixed in 2.5% w/v formaldehyde and 3% w/v sucrose in phosphate buffered saline (PBS) for one hour. The tissues were washed three times with PBS for 20 min each, followed by a 10 min wash of 1:3 glycerol:PBS and a 10 min wash of 1:1 glycerol:PBS. The tissue was then immersed in glycerol and mounted between two glass cover slips that were sealed with clear nail polish around the edge to a 100 μ m-thick aluminum microscope slide with a 1 cm-diameter hole punched in the center.

The recently fixed preparations were imaged with a Leica SP2 multiphoton scanning laser microscope at the W.M. Keck Bioimaging Lab at Arizona State University. We excited the tissues with a 488 nm

wavelength argon laser at 49% power setting and observed the auto-fluorescent emissions in the 489–508 nm window through a 40 \times oil-immersion objective. Images (0.375 mm²) were recorded digitally with an image size of 2048 \times 2048 pixels and with 2 μ m steps in the z-axis.

2.5. Confocal microscopy image analysis

The image stacks recorded with confocal microscopy were transformed into projection images in ImageJ 1.37v (Wayne Rasband, NIH, USA, Fig. 3). Adjacent projections were tiled together in Adobe Photoshop and levels were adjusted to maintain uniform background. Regions in which large tracheae, cuticle, or other aberrations appear were discarded. For each individual, a grid was superimposed on the

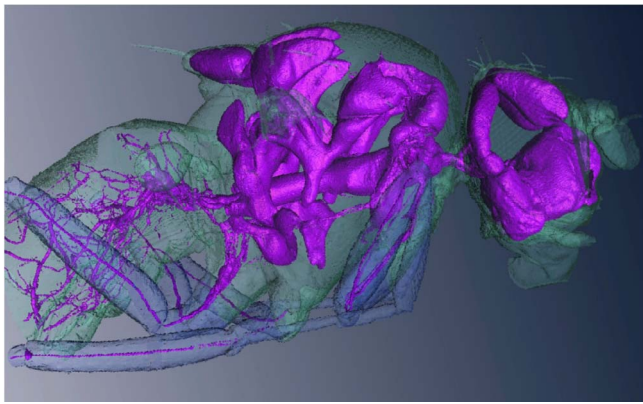


Fig. 2. Air sacs (purple) within a *Drosophila melanogaster*, visualized using SR- μ CT.

projection, and 25 squares ($625 \mu\text{m}^2$ each) that covered the flight muscle were randomly selected. The collection of grids was imported to ImageJ as an image stack, converted to 8-bit grayscale and then converted into binary using a standard threshold level. To find the area density of tracheal structures for each image in the sequence, we determined the proportion of pixels in each frame that contained tracheal structures (which are a mix of tracheae and tracheoles).

For five normoxic-reared flies for which we had particularly high-quality images, we were able to measure the effect of tracheal generation number on the dimensions of the tracheae out to generation 5. We randomly selected one branch per generation per tree and measured the length and diameter of that tracheal branch with ImageJ. For two of the trees, image quality allowed us to be able to count the number of branches per generation. Branching was approximately dichotomous, so we estimated the total longitudinal oxygen diffusing capacity of each generation as the diffusing capacity of the tracheal branch (see calculation below) times the estimated number of branches per generation (generation 0 = 1, generation 1 = 2, ... generation 5 = 32).

To test the effect of rearing oxygen on the dimensions of the tracheae observed with confocal microscopy, we used ImageJ to measure the lengths and diameters of generations 0–2 of tracheal trees (Fig. 3). Generation 0 was defined as the largest tracheal trunk of a well-imaged tree; we only chose trees for which the start of generation 0 could be observed, allowing us to calculate a length. Beyond the 2nd generation of tracheal branches, we could not reliably trace tracheoles in sufficient number of animals to test the effect of oxygen. Because the diameters varied along the length of a branch, especially for generations 0 and 1, we traced the 2D area of each branch and divided by branch length to calculate average cross-sectional diameter. Because we had a nested

design and the number of tracheal trees available to measure varied among individuals, to maintain a balanced statistical design, we restricted the number of branches to three per individual per generation, with the branches chosen for measurement selected randomly.

The capacity of a tracheal branch to conduct oxygen axially down the length of the branch (G , $\text{nmol kPa}^{-1}\text{s}^{-1}$) was calculated as:

$$G = D \cdot \beta \cdot A / L \quad (1)$$

with D (the diffusion constant for O_2 in air at 25°C) = $0.178 \text{ cm}^2 \text{ s}^{-1}$ (Lide, 1991), β (the capacitance for oxygen in air, $1/RT$) = $404 \text{ nmol cm}^{-3}\text{kPa}^{-1}$ (Piiper et al., 1971), A = cross-sectional area (cm^2) and L = length (cm).

2.6. Statistical analyses

Most statistical analysis were conducted in R (R-Core-Team, 2016). Data were first tested for normality using the Shapiro-Wilks test and for homoscedasticity using Bartlett's test; parametric tests were only performed on data that met these assumptions. Effects of rearing oxygen on parameters of the tracheal system measured with SR- μ CT were generally tested using ANOVA, or the relevant nonparametric test. For the confocal images, we analyzed data using a linear mixed effects model, using animal and generation as nested random effects and specifying rearing oxygen level as a fixed effect using the lme function in the nlme package in R (Pinheiro et al., 2017). Effects of oxygen on thorax length were tested using an equality of medians test using STAT 14.2. All tests were two-tailed, with $P \leq 0.05$ taken to indicate statistical significance.

3. Results

3.1. Effects of rearing oxygen level on size, flight muscles, and tracheae as imaged with SR- μ CT

Overall, there was a tendency for flies in both hypoxia and hyperoxia to be smaller than those reared in normoxia (Fig. 4). Thorax lengths were not distributed normally and could not be transformed to normal. Rearing oxygen level significantly affected thorax length (equality of median's test, $\chi^2_2 = 7.23$, $P = 0.027$). Rearing P_{O_2} levels significantly affected flight muscle volume (one-way ANOVA, $F_{2,28} = 4.71$, $P = 0.018$), with flies reared at 40 kPa having smaller muscle fibers than 21 kPa-reared, but no other significant differences among groups were observed (Scheffe's post hoc test).

The main finding for the morphology of the larger tracheae as visualized by SR- μ CT was that there was no evidence for enlargement of tracheae at lower rearing oxygen levels. Rearing oxygen significantly affected the number of secondary tracheal branches, with the 10 kPa-

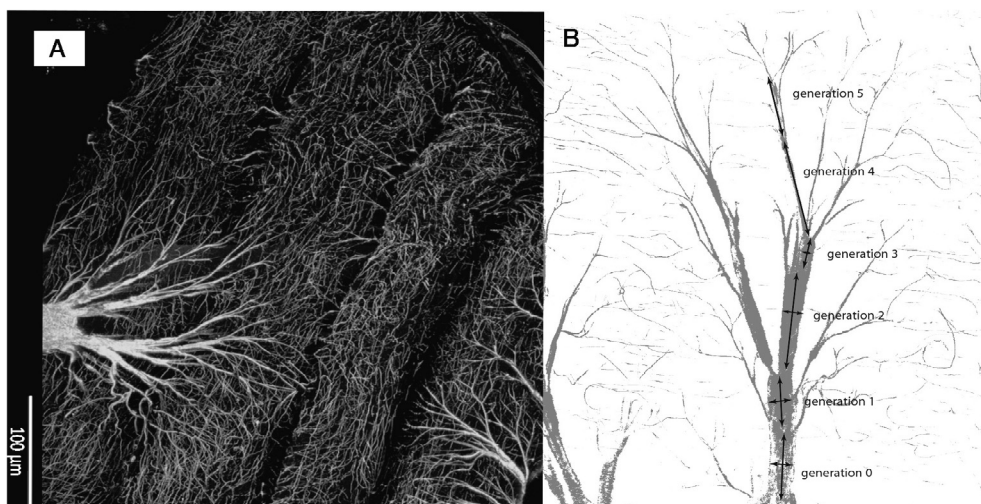


Fig. 3. A: Confocal image of the tracheolar supply to the dorsolongitudinal flight muscles. The lighter tree-like structure is extracellular; most of the tracheoles are intracellular, running longitudinally within the flight muscle fibers. B: A single tracheal branch, with branch generations labeled.

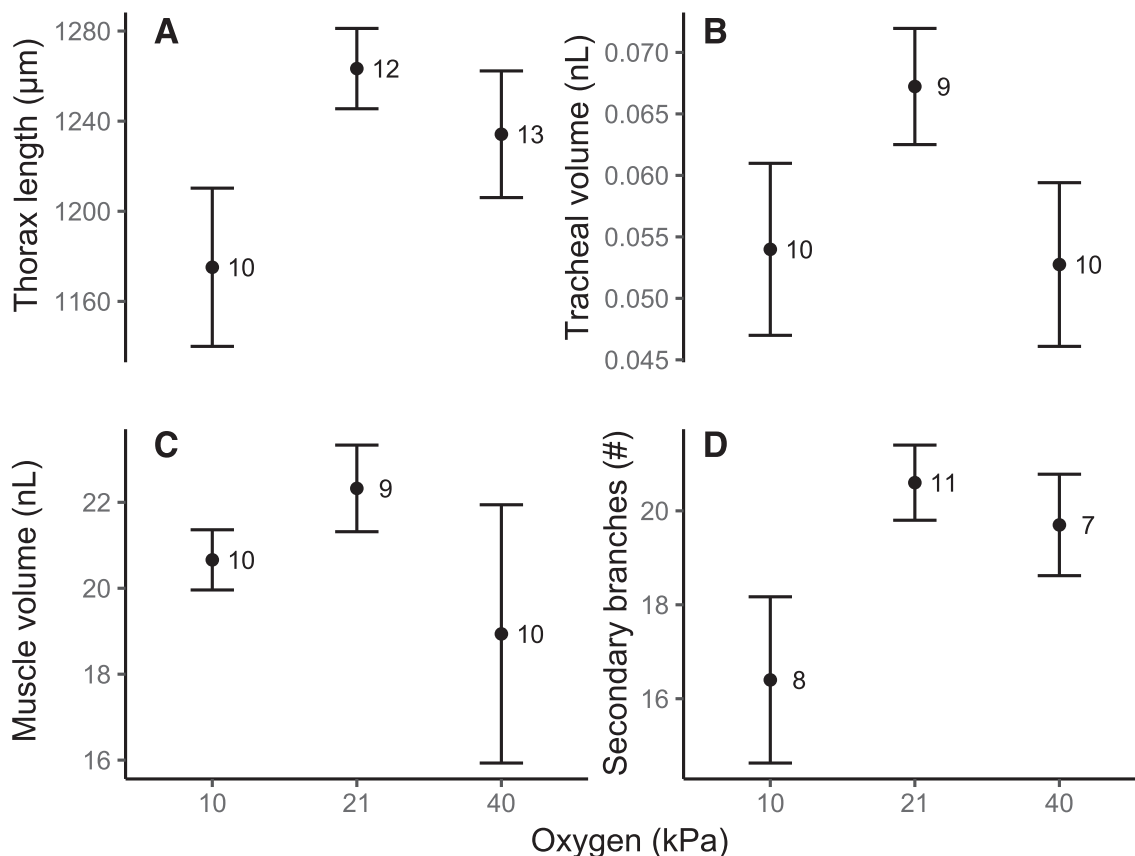


Fig. 4. The effect of oxygen level on: A: thorax length (Kruskal-Wallis rank test, $P = 0.014^*$); B: volume of the secondary and tertiary right ventro-lateral flight muscle trachea (NS); C: volume of the four most ventral right dorsolongitudinal flight muscles (one-way ANOVA, $F_{2,28} = 4.71$, $P = 0.018^*$); D: number of secondary branches (ANOVA, $F_{2,26} = 3.44$, $P = 0.048^*$). Mean \pm s.e.m. shown. Sample sizes (number of animals) shown next to each symbol. For this and subsequent figures: NS = nonsignificant, * = significant, $P < 0.05$.

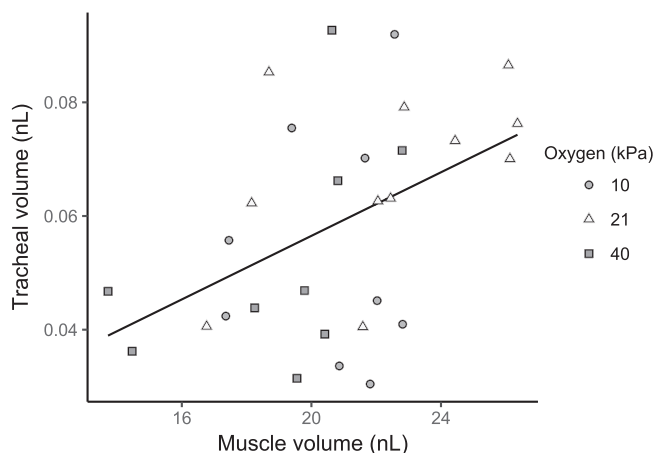


Fig. 5. Flies with larger flight muscles had larger volumes of the combined secondary and tertiary right ventro-lateral flight muscle tracheae (RVLMT, linear regression, $F_{1,27} = 7.01$, $r^2 = 0.21$, $P = 0.013^*$; 95% confidence interval shown, $n = 29$). Oxygen rearing level did not affect tracheal volumes after controlling for muscle volume (each symbol is one individual, linear regression, NS). Squares: 10 kPa-reared, Circles: 21 kPa-reared, Triangles: 40 kPa-reared.

reared flies having fewer branches (Fig. 4, ANOVA, $F_{2,26} = 3.44$, $P = 0.048$). Rearing oxygen level did not significantly affect the volume of the secondary and tertiary tracheae of the RVLMT (Fig. 4, ANOVA, $F_{2,28} = 2.94$, $P = 0.071$). Rearing oxygen level also did not significantly affect the length of all RVLMT tracheae (ANOVA, $P = 0.39$), the number of tertiary tracheae (ANOVA, $P = 0.69$), or the number of side branches (Kruskal-Wallis, $P = 0.17$). Flies with larger muscle volumes had larger tracheal volumes (Fig. 5, all oxygen

Table 1

Summary table for morphological characters measured of *Drosophila* used in the SR- μ CT study. Values for tracheae refer to the right ventro-lateral flight muscle trachea (RVLMT, Fig. 1), and values for the flight muscles refer to the right-side dorsal-longitudinal flight muscles (DLFM) identified as 1–4 in Fig. 1. Animals were pooled across oxygen treatments as these mostly did not significantly affect morphology.

Parameter	Mean	s.e.m.	Range
Head width, μm	724	9.5	584–790
Thorax length, μm	911	13.6	737–1064
Secondary tracheal branches, number	19.1	0.75	10–25
Tertiary tracheal branches, number	18.1	1.42	5–27
Side tracheal branches, number	5.7	0.44	3–14
Total tracheal branches, number	42.9	2.04	24–58
Total length of all branches, mm	17.7	1.02	5.8–25.6
Total volume of secondary and tertiary tracheae, pL	72.5	4.44	38–115
Total volume of 4DLFM fibers served, nL	25.6	0.72	17–33

treatments pooled, linear regression, $F_{1,27} = 7.01$, $r^2 = 0.21$, $P = 0.013$), and including oxygen treatment groups as predictor variables did not significantly improve the model (linear regression ANCOVA, $P = 0.45$). The average RVLMT had a total of 43 secondary, tertiary, and side branches adding up to about 17 mm in length (Table 1).

3.2. Effects of rearing oxygen level on flight muscle tracheae imaged with confocal microscopy

The tracheae visualized with confocal microscopy served the upper myofibers of the DLFM (Fig. 3). The largest tracheae visible here (generation 0) was likely equivalent to the secondary inter-fiber tracheae, as these were comparable to the secondary tracheae measured in

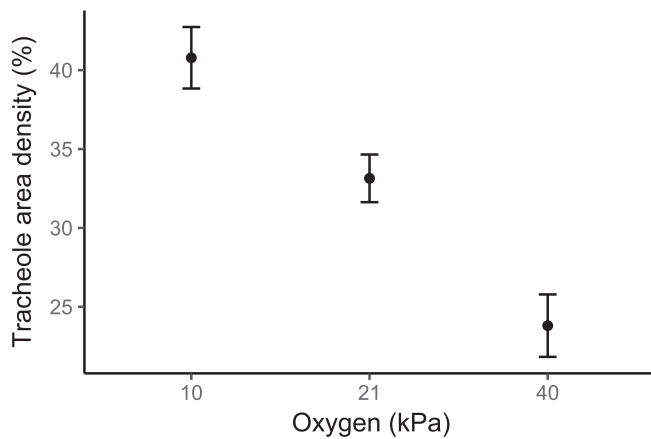


Fig. 6. Effect of rearing oxygen level on the area density of tracheal structures in flight muscle (area density measured as% of a 2D projection confocal image of flight muscle occupied by tracheal structures; oneway ANOVA, $F_{1, 13} = 46.31$, $P < 0.001^*$, $n = 15$).

the SR- μ CT study both in location and diameter. After three to four generations of branching (sometimes only one), diameters of the tracheal structures were less than 2 μ m and had penetrated into the flight muscle fibers, and thus were likely tracheoles.

There was a strong compensatory response to rearing oxygen level observed in the area density of tracheal structures. The percentage of the 2D projection images of flight muscle that contained tracheae or tracheoles declined from 41 to 24% as rearing oxygen rose from 10 to 40 kPa (Fig. 6; $F_{1,13} = 46.31$, $P < 0.001$). Because the confocal analysis was conducted on 2D projection images that combine information from 3D structures, actual densities of tracheal structures in the tissues are much less. This imaging effect resulted from the finite depth of illumination of the laser. The intensity of fluorescence dropped substantially from confocal optical slices more than 50 μ m in depth, so we assume 50 μ m to be the total tissue depth. In the z-axis, we had a slice every 2 μ m, thus our 2D projection images were composed of 25 2D slices, so to estimate the actual 3D tracheal densities in the flight muscles, we divided the area densities from the 2D projection images by 25. Using this method, actual densities of tracheal structures in the flight muscle were calculated to decline from 1.6 to 1% as the rearing oxygen level increased from 10 to 40 kPa rearing oxygen. With the linear, mixed effects model, using generation as a nested random effect, branch lengths were significantly affected by rearing oxygen (Fig. 7, $F_{2,55} = 6.44$, $P = 0.003$), with the flies reared in 10 kPa oxygen having significantly shorter branch lengths than the normoxic-reared flies ($t_{1,17} = 2.73$, $P = 0.014$). However, using this same statistical approach, diameters and axial diffusing capacities of the tracheae were not significantly affected by rearing oxygen.

We analyzed the effect of generation number on the dimensions of the tracheae for the flies reared in normoxia. Branch diameter decreased successively with generation after generation 1, but branch length was relatively constant (Fig. 8). The axial diffusing capacity of all the tracheae in a generation of a tree decreased more than 10-fold from generation 0–5 (Fig. 8).

4. Discussion

Rearing *D. melanogaster* in 10 or 40 kPa oxygen resulted in strong compensatory changes in density of the tracheoles of the flight muscles, but no compensatory morphological changes in the large tracheae supplying the flight muscles. These results support the hypothesis that morphological responses to rearing in low or high oxygen environments primarily occur in parts of the tracheal system that are distal from the spiracles and/or not well-ventilated.

These conclusions are supported by the findings of a complementary study (VandenBrooks et al., 2017), which also found compensatory

changes in branching in tracheoles within *Drosophila* flight muscle for animals reared in hypoxia or hyperoxia. Vandenbrooks et al. showed that the diameters of tracheoles were larger in *Drosophila* reared at 12 kPa P_{O_2} relative to 21 kPa P_{O_2} , and smaller in flies reared at 31 kPa P_{O_2} . Vandenbrooks et al. reported tracheolar diameters within the flight muscles that ranged from 0.15 to 0.35 μ m, and changes due to rearing oxygen level in the range of 0.07 μ m. These sizes were broadly consistent with our measurements, but our resolution of 0.18 μ m/pixel was insufficient to assess such diameter changes.

The main tracheal trunk of the RVLfMT and all of the air sacs appear compressible (Figs. 1 and 2), and it is likely that it and other tracheal structures are ventilated tidally by pressure changes associated with the pumping proboscis during flight, which is correlated with bursts of CO_2 emission during flight (Lehmann and Heymann, 2005) and air sac compression in the head (Westneat et al., 2008). It is unclear whether the more distal tracheae and tracheoles are compressed and ventilated during the tidal ventilation driven by this pumping of the proboscis or other processes (e.g., autoventilation associated with flight muscle contractions). Resolving this question of tracheal compression throughout the body is necessary for development of a quantitative model of gas transport for oxygen transport in insects.

Our data are consistent with other studies that suggest that rearing in either 10 or 40 kPa oxygen at 25 $^{\circ}C$ is stressful for *D. melanogaster*, as both treatments resulted in reduced thoracic size or flight muscle volume. Rearing in 10 kPa oxygen has consistently been shown to reduce adult mass, while 40 kPa oxygen has been shown to either increase or have no effect on adult mass (Frazier et al., 2001; Heinrich et al., 2011; Klok et al., 2009; Klok et al., 2016; Peck and Maddrell, 2005). However, both 10 and 40 kPa oxygen have been shown to reduce rates of larval growth and feeding (Farzin et al., 2014). In adult flies, 10 kPa oxygen can reduce or extend longevity, while 40 kPa oxygen atmospheres consistently reduce longevity (Charette et al., 2011; Rascón and Harrison, 2010). However, effects of 40 kPa oxygen may be more beneficial at higher body temperatures, resulting from the strong and exponential effects of temperature on oxygen consumption rate (Frazier et al., 2001).

It has been shown in some insects that the axial diffusing capacity or summed cross-sectional area of successive generations is constant, allowing development of simple models of gas diffusion for insects (Krogh, 1920; Locke, 1958; Thorpe and Crisp, 1947). In contrast, we found that, for the tracheae next to and within the flight muscle, the axial diffusing capacity decreases strongly with each successive generation (Fig. 8). The cited prior studies that found constant summed cross-sectional areas across generations focused on larger tracheae. We hypothesize that preservation of summed cross-sectional area and axial diffusing capacity across generations is a feature of regions of the tracheal system where transport of oxygen laterally across the tracheal wall is minimal. Within the region of the flight muscle, oxygen is both diffusing axially down the tracheae as well as laterally across the tracheolar walls into tissue. Based on TEM studies that included measures of the area and thickness of tracheal walls, the smallest tracheoles have by far the majority of the lateral diffusing capacity (Hartung et al., 2004; Schmitz and Perry, 1999; Snelling et al., 2011, 2012). Thus, we predict that, for all insects, in regions with high lateral diffusing capacity and substantial oxygen transport to tissues, there will be a systematic decrease in axial diffusing capacities with generation. Combining volumetric imaging techniques such as confocal or CT with TEM studies will be necessary to test this hypothesis, as measurements of the wall thickness of the tracheal system are required to measure lateral diffusing capacities.

Our conclusions about declining axial diffusing capacities with generation are somewhat tempered by limits on the resolution of our confocal images. Our pixel sizes were 0.18 μ m, and our measurements suggested that the smallest tracheoles approached 0.3 μ m in diameter, too small for us to measure accurately. Up to generation 2, the vast majority of tracheae had diameters greater than 1 μ m, representing 5 or

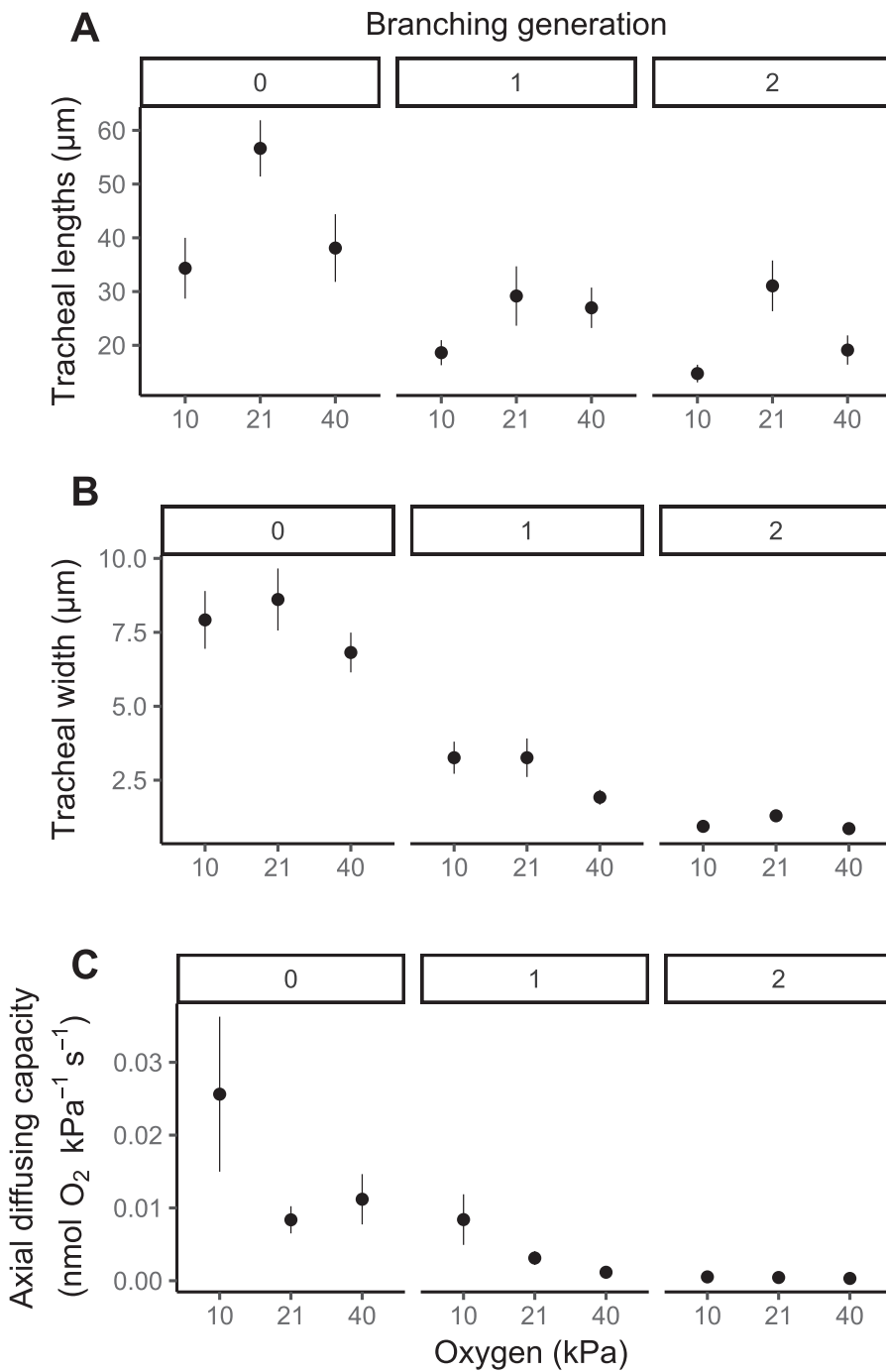


Fig. 7. Effect of rearing oxygen level on the dimensions and axial diffusing capacities of the tracheae assessed with confocal microscopy. Rearing oxygen level significantly decreased branch lengths in hypoxic-reared flies, consistent with increased branching and proliferation of tracheoles in hypoxia (linear mixed effects model, $F_{2,55} = 6.44$, $P = 0.003$; 9, 5 and 6 flies at 10, 21 and 40 kPa, respectively, with three branches measured for three generations of tracheal branches).

more pixels in the image. However, for generations 4 and 5 of the normoxic reared flies, tracheolar diameters diminished to sizes that approached 2–4 pixels, so these reported values have a higher measurement uncertainty.

The correlation between flight muscle volume and the volume of the major tracheae supplying this muscle (Fig. 4) emphasizes the developmental necessity for animals to match oxygen supply to demand as they develop, and across body size among individuals. Similarly, the lateral diffusing capacity of the tracheal system in muscle was tightly matched to variation in mitochondrial volumes across body size in grasshoppers (Snelling et al., 2011, 2012). Because inadequate oxygen supply can limit ATP production and the capacity to grow, move and reproduce, there should be strong selection to maintain adequate oxygen delivery capacities as animals grow, and across animals of

different sizes. The selective factors that ensure that tracheal development is not excessive are less clear, but may include material and space costs (e.g. more tracheae means less space for contractile systems in muscle) and possibly a need to reduce tracheation to ensure that the partial pressures of oxygen in tissues are not excessive, as elevated tissue P_{O_2} may promote reactive oxygen species and oxidative damage (Hetz and Bradley, 2005). The observation that the percent of tracheal space within muscle is relatively small (estimated as about 1%, this study, and by (Snelling et al., 2011, 2012)) provides some cautious evidence for the hypothesis that tracheation is reduced in hyperoxia to reduce oxidative damage. The matching of tracheal morphology to tissue need during development is likely accomplished by multiple interacting mechanisms including morphogen gradients that index tissue size (Amourda and Saunders, 2017), and secretion of growth factors by

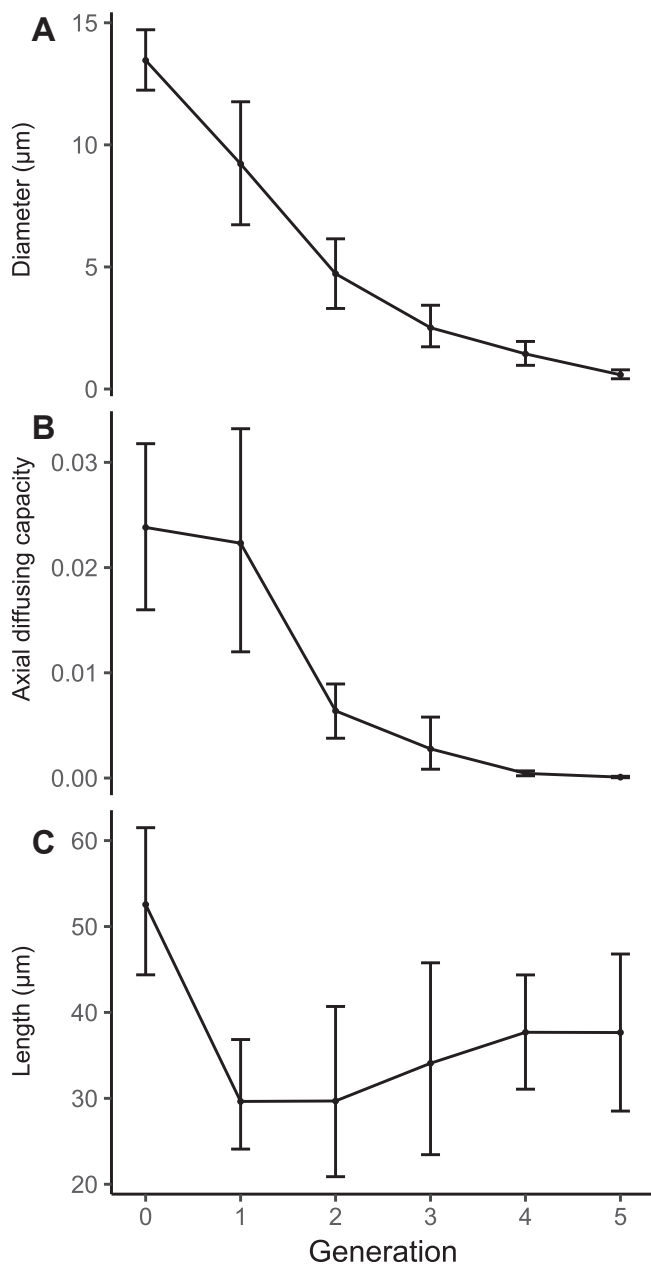


Fig. 8. Effect of generation number on diameters (A, ANOVA^{*}), axial oxygen diffusing capacity (B, ANOVA^{*}, nmol·kPa⁻¹·s⁻¹), and lengths (C, NS) for normoxic-reared flies (five flies, one branch measured for six generations of tracheal branches).

oxygen-consuming tissues that regulate tracheal growth (Ghabrial et al., 2003). Integrating organismal studies of the tracheal system structure and function with molecular developmental approaches is necessary to understand the mechanisms responsible for stability and plasticity of different components of the tracheal system when oxygen availability varies.

In general, these tomographic and confocal approaches are complementary, enabling new insight into tracheal system design and function. The tomographic approaches are particularly noteworthy for the excellent visualization provided for regions or entire systems of tracheae. With more classical manual microscopic measurements, we are often limited by technical or time limitations to measurements of a few straight tracheae, which are not fully representative of the system as a whole. In contrast, tomography provides rich 3D datasets, enabling measurements such as summed tracheal system volume or the length of all tracheae within a region of interest to better evaluate an integrated,

whole-system response. However, compared to classical microscopy, there is greater uncertainty about the limits of resolution of tomography as tracheal diameters approach the size of individual voxels. Rigorous quantitative study is needed to characterize such factors as phase enhancement and numerous reconstruction parameters on the ability to visualize the smallest tracheoles in various types of tissue. While confocal microscopy approaches to assessing tracheoles have been used by developmental biologists for some time, most prior quantitative physiological studies of tracheoles have used electron microscopy. Major advantages of the confocal approaches are much quicker tissue preparation, lack of concern of shrinkage or deformation associated with fixation, visualization of regions of tracheae in three dimensions, and the ability to measure tracheolar lengths. Disadvantages (or advantages to electron microscopy) include the fact that confocal microscopy has a limited capacity to visualize deep tissue, and in some cases the system resolution may be insufficient to measure diameters of small tracheoles or their wall thickness. However, technical improvements in both X-ray tomography and confocal microscopy promise to overcome many of these issues, and these imaging approaches should enable rapid progress in our understanding of tracheal system structure and function.

Acknowledgements

Use of the Advanced Photon Source, an Office of Science User Facility operated for the U.S. Department of Energy (DOE) Office of Science by Argonne National Laboratory, was supported by the U.S. DOE under Contract No. DE-AC02-06CH11357. Francesco De Carlo, Xianghui Xiao, Kamel Fezzaa, and Wah-Keat Lee were especially helpful with developing protocols for synchrotron x-ray imaging, and Xianghui Xiao and Francesco De Carlo performed the three-dimensional reconstructions of the SR-µCT images. We thank Elizabeth Lee for help with Fig. 2. Carsten Duch, Claudia Kuehn, Fernando Vonhoff, and Erin McKiernan taught us how to dissect *Drosophila* flight muscle. Robert Roberson, Douglas Chandler, David Lowry, Bret Judson, and Deborah Baluch were instrumental in supporting our use of the Keck Bioimaging Facility at Arizona State University. The manuscript was substantially improved by the comments of two anonymous reviewers. This research was supported by NSF IOS 1122157, NSF IOS 0419704 to J.F.H., and NSF EFRI 0938047 and NSF IOS 1558052 to J.J.S. and J.F.H.

Appendix A. Supplementary data

Supplementary data associated with this article can be found, in the online version, at <http://dx.doi.org/10.1016/j.jinsphys.2017.09.006>.

References

- Acevedo, J.M., Centanin, L., Dekanty, A., Wappner, P., 2010. Oxygen sensing in *Drosophila*: multiple isoforms of the prolyl hydroxylase fatiga have different capacity to regulate HIFα/Sima. *PLoS ONE* 5, e12390.
- Amourda, C., Saunders, T.E., 2017. Gene expression boundary scaling and organ size regulation in the *Drosophila* embryo. *Dev. Growth Differ.* 59, 21–32.
- Callier, V., Hand, S.C., Campbell, J.B., Biddulph, T., Harrison, J.F., 2015. Developmental changes in hypoxic exposure and responses to anoxia in *Drosophila melanogaster*. *J. Exp. Biol.* 218, 2927–2934.
- Callier, V., Nijhout, H.F., 2014. Plasticity of insect body size in response to oxygen: integrating molecular and physiological mechanisms. *Curr. Opin. Insect Sci.* 1, 59–65.
- Centanin, L., Gorr, T.A., Wappner, P., 2010. Tracheal remodelling in response to hypoxia. *J. Insect. Physiol.* 56, 447–454.
- Charette, M., Darveau, C.-A., Perry, S.F., Rundle, H.D., 2011. Evolutionary consequences of altered atmospheric oxygen in *Drosophila melanogaster*. *PLoS ONE* 6, e26876.
- Dickinson, M.H., Lighton, J.R.B., 1995. Muscle efficiency and elastic storage in the flight motor of *Drosophila*. *Science* 268, 87–90.
- Dillon, M.E., Dudley, R., 2014. Surpassing Mt. Everest: extreme flight performance of alpine bumble-bees. *Biol. Lett.* 10.
- Dowd, B.A., Campbell, G.H., Peter Siddons, D.P., Marr, R.B., Nagarkar, V., Tipnis, S., Axe, L., 1999. Developments in synchrotron X-ray computed microtomography at the National Synchrotron Light Source. *Proc. SPIE* 3772, 224–236.
- Farzin, M., Albert, T., Pierce, N., Vandenbrooks, J.M., Dodge, T., Harrison, J.F., 2014. Acute and chronic effects of atmospheric oxygen on the feeding behavior of *Drosophila melanogaster* larvae. *J. Insect Physiol.* 68, 23–29.

- Frazier, M.R., Woods, H.A., Harrison, J.F., 2001. Interactive effects of rearing temperature and oxygen on the development of *Drosophila melanogaster*. *Physiol. Biochem. Zool.* 74, 641–650.
- Ghabrial, A., Luschnig, S., Metzstein, M.M., Krasnow, M.A., 2003. Branching morphogenesis of the *Drosophila* tracheal system. *Annu. Rev. Cell Dev. Biol.* 19, 623–647.
- Harrison, J., Frazier, M.R., Henry, J.R., Kaiser, A., Klok, C.J., Rascon, B., 2006. Responses of terrestrial insects to hypoxia or hyperoxia. *Respir. Physiol. Neurobiol.* 154, 4–17.
- Harrison, J.F., Philips, J.E., Gleeson, T.T., 1991. Activity physiology of the two-striped grasshopper, *Melanoplus bivittatus*: gas exchange, hemolymph acid-base status, lactate production and the effect of temperature. *Physiol. Zool.* 64, 451–472.
- Harrison, J.F., Wasserthal, L.T., Chapman, R.F., 2013a. Gaseous exchange. In: Simpson, S.J., Douglas, A.E. (Eds.), *The Insects: Structure and Function*, fifth ed. Cambridge University Press, New York, pp. 501–545.
- Harrison, J.F., Waters, J.S., Cease, A.J., VandenBrooks, J.M., Callier, V., Klok, C.J., Shaffer, K.M., Socha, J.J., 2013b. How locusts breathe. *Physiology* 28, 18–27.
- Hartung, D.K., Kirkton, S.D., Harrison, J.F., 2004. Ontogeny of tracheal system structure: a light and electron-microscopy study of the metathoracic femur of the American locust, *Schistocerca americana*. *J. Morphol.* 262, 800–812.
- Heinrich, E.C., Farzin, M., Klok, C.J., Harrison, J.F., 2011. The effect of developmental stage on the sensitivity of cell and body size to hypoxia in *Drosophila melanogaster*. *J. Exp. Biol.* 214, 1419–1427.
- Henry, J.R., Harrison, J.F., 2004. Plastic and evolved responses of larval tracheae and mass to varying atmospheric oxygen content in *Drosophila melanogaster*. *J. Exp. Biol.* 207, 3559–3567.
- Hetz, S.K., Bradley, T.J., 2005. Insects breathe discontinuously to avoid oxygen toxicity. *Nature* 433, 516–519.
- Heymann, N., Lehmann, F.-O., 2006. The significance of spiracle conductance and spatial arrangement for flight muscle function and aerodynamic performance in flying *Drosophila*. *J. Exp. Biol.* 209, 1662–1677.
- Hoback, W.W., Stanley, D.W., 2001. Insects in hypoxia. *J. Insect. Physiol.* 47, 533–542.
- Huang, S.-P., Sender, R., Gefen, E., 2014. Oxygen diffusion limitation triggers ventilatory movements during spiracle closure when insects breathe discontinuously. *J. Exp. Biol.* 217, 2229–2231.
- Jarecki, J., Johnson, E., Krasnow, M.A., 1999. Oxygen regulation of airway branching in *Drosophila* is mediated by branchless FGF. *Cell* 99, 211–220.
- Klok, C.J., Hubb, A.J., Harrison, J.F., 2009. Single and multigenerational responses of body mass to atmospheric oxygen concentrations in *Drosophila melanogaster*: evidence for roles of plasticity and evolution. *J. Evol. Biol.* 22, 2496–2504.
- Klok, C.J., Kaiser, A., Socha, J.J., Lee, W.K., Harrison, J.F., 2016. Multigenerational effects of rearing atmospheric oxygen level on the tracheal dimensions and diffusing capacities of pupal and adult *Drosophila melanogaster*. In: Roach, R.C., Wagner, P.D., Hackett, P.H. (Eds.), *Hypoxia*. Springer, New York.
- Krogh, A., 1920. Studien über Tracheenrespiration. II. über Gasdiffusion in den Tracheen. *Pflügers Archiv.* 179, 95–112.
- Lavista-Llanos, S., Centanin, L., Irisarri, M., Russo, D.M., Gleadle, J.M., Bocca, S.N., Muzzopappa, M., Ratcliffe, P.J., Wappner, P., 2002. Control of the hypoxic response in *Drosophila melanogaster* by the basic helix-loop-helix PAS protein similar. *Mol. Cell Biol.* 22, 6842–6853.
- Lehmann, F.-O., 2001. Matching spiracle opening to metabolic need during flight in *Drosophila*. *Science* 294, 1926–1929.
- Lehmann, F.-O., Dickinson, M.H., 1997. The changes in power requirements and muscle efficiency during elevated force production in the fruit fly *Drosophila melanogaster*. *J. Exp. Biol.* 200, 1133–1143.
- Lehmann, F.O., Heymann, N., 2005. Unconventional mechanisms control cyclic respiratory gas release in flying *Drosophila*. *J. Exp. Biol.* 208, 3645–3654.
- Lide, D.R., 1991. *CRC Handbook of Chemistry and Physics*, 72 ed. CRC Press, Boca Raton.
- Locke, M., 1958. The co-ordination of growth in the tracheal system of insects. *Q. J. Microsc. Sci.* 99, 373–391.
- Loudon, C., 1989. Tracheal hypertrophy in mealworms: design and plasticity in oxygen supply systems. *J. Exp. Biol.* 147, 217–235.
- Marden, J.H., Fescemyer, H.W., Schilder, R.J., Doerfler, W.R., Vera, J.C., Wheat, C.W., 2012. Genetic variation in HIF signaling underlies quantitative variation in physiological and life-history traits within lowland butterfly populations. *Evolution* 67, 1105–1115.
- Meyer, E.P., 1989. Corrosion casts as a method for investigation of the insect tracheal system. *Cell Tissue Res.* 256, 1–6.
- Peck, L.S., Maddrell, S.H.P., 2005. Limitation of size by hypoxia in the fruit fly *Drosophila melanogaster*. *J. Exp. Zool. A Comp. Exp. Biol.* 303A, 968–975.
- Piiper, J., Dejours, P., Haab, P., Rahn, H., 1971. Concepts and basic quantities in gas exchange physiology. *Respir. Physiol.* 13, 292–304.
- Pinheiro, J., Bates, D., DebRoy, S., Sarkar, D., Team, R.C., 2017. nlme: linear and non-linear mixed effects models, R package version 3.1-131.
- R-Core-Team, 2016. R: A language and environment for statistical computing. R Foundation for Statistical Computing, Vienna, Austria.
- Rascón, B., Harrison, J.F., 2010. Lifespan and oxidative stress show a nonlinear response to atmospheric oxygen level in *Drosophila*. *J. Exp. Biol.* 213, 3441–3448.
- Scheidt, P., Hook, C., Bridges, C.R., 1981. Diffusion in Gas Exchange of Insects. *Fed. Proc.* 41, 2143–2145.
- Schmitz, A., Harrison, J.F., 2004. Hypoxic tolerance in air-breathing invertebrates. *Respir. Physiol. Neurobiol.* 141, 229–242.
- Schmitz, A., Perry, S.F., 1999. Stereological determination of tracheal volume and diffusing capacity of the tracheal walls in the stick insect *Carausius morosus* (Phasmatodea, Lonchodidae). *Physiol. Biochem. Zool.* 72, 205–218.
- Snelling, E.P., Seymour, R.S., Runciman, S., Matthews, P.G.D., White, C.R., 2011. Symmorphosis and the insect respiratory system: allometric variation. *J. Exp. Biol.* 214, 3225–3237.
- Snelling, E.P., Seymour, R.S., Runciman, S., Matthews, P.G.D., White, C.R., 2012. Symmorphosis and the insect respiratory system: a comparison between flight and hopping muscle. *J. Exp. Biol.* 215, 3324–3333.
- Socha, J.J., DeCarlo, F., 2008. Use of synchrotron tomography to image naturalistic anatomy in insects. *SPIE* 2008, 70780A–70787.
- Socha, J.J., Forster, T.D., Greenlee, K.J., 2010. Issues of convection in insect respiration: insights from synchrotron X-ray imaging and beyond. *Respir. Physiol. Neurobiol.* 173S, S65–S73.
- Thorpe, W.H., Crisp, D.J., 1947. Studies on plastron respiration. I. The biology of *Aphelocheirus* (Hemiptera, Aphelocheiridae (Naucoridae)) and the mechanism of plastron respiration. *J. Exp. Biol.* 24, 227–269.
- VandenBrooks, J.M., Gstrein, G., Harmon, J., Friedman, J., Olsen, M., Ward, A., Parker, G., 2017. Supply and demand: How does variation in atmospheric oxygen affect insect tracheal and mitochondrial networks? *J. Insect. Physiol.*
- VandenBrooks, J.M., Munoz, E.E., Weed, M.D., Ford, C.F., Harrison, M.A., Harrison, J.F., 2012. Impacts of paleo-oxygen levels on the size, development, reproduction, and tracheal systems of *Blattella germanica*. *Evol. Biol.* 39, 83–93.
- Westneat, M.W., Socha, J.J., Lee, W.K., 2008. Advances in biological structure, function and physiology using synchrotron X-ray imaging. *Annu. Rev. Physiol.* 70, 119–142.
- Whitten, J., 1957. The post-embryonic development of the tracheal system in *Drosophila melanogaster*. *J. Microsc. Sci.* 98, 123–150.
- Wigglesworth, V.B., 1983. The physiology of insect tracheoles. *Adv. Insect. Physiol.* 17, 85–149.